Nano Energy 29 (2016) 126–135

Contents lists available at ScienceDirect

Nano Energy

journal homepage: www.elsevier.com/locate/nanoen

Beyond the top of the volcano? – A unified approach to electrocatalytic oxygen reduction and oxygen evolution

Michael Busch [a,c], Niels B. Halck [b,c], Ulrike I. Kramm [d], Samira Siahrostami [c,e], Petr Krtil [f], Jan Rossmeisl [g,*]

[a] Laboratory for Computational Molecular Design (LCMD) and National Center for Computational Design and Discovery of Novel Materials (MARVEL), École Polytechnique Fédérale de Lausanne, Station 12, 1015 Lausanne, Switzerland
[b] Department of Energy Conversion and Storage, Technical University of Denmark, Frederiksborgvej 399, DK-4000 Roskilde, Denmark
[c] Department of Physics, Technical University of Denmark, Fysikvej Building 311, DK-2800 Kongens Lyngby, Denmark
[d] Department of Chemistry and Department of Materials, and Earth Science, Technical University of Darmstadt, Jovanka-Bontschits-Str. 2, 64287 Darmstadt, Germany
[e] Department of Chemical Engineering, Stanford University, Stanford, CA 94305, United States
[f] J. Heyrovsky Institute of Physical Chemistry, Academy of Sciences of the Czech Republic, Dolejskova 3, CZ-18223 Prague, Czech Republic
[g] Department of Chemistry, Nano-Science Center, University of Copenhagen, Universistetsparken 5, DK-2100 København Ø., Denmark

ARTICLE INFO

Article history:
Received 25 November 2015
Received in revised form
8 April 2016
Accepted 9 April 2016
Available online 22 April 2016

Keywords:
Electrocatalysis
Oxygen reduction
Oxygen evolution
Volcano
Density functional theory

ABSTRACT

We study the oxygen reduction (ORR) and the oxygen evolution reaction (OER) and based on previous obtained mechanistic insight we provide a unified general analysis of the two reactions simultaneously. The analysis shows that control over at least two independent binding energies is required to obtain a reversible perfect catalyst for both ORR and OER. Often only the reactivity of the surface is changed by changing from one material to another and all binding energies scale with the reactivity. We investigate the limitation in efficiency imposed by these linear scaling relations. This analysis gives rise to a double volcano for ORR and OER, with a region in between, forbidden by the scaling relations. The reversible perfect catalyst for both ORR and OER would fall into this "forbidden region". Previously, we have found that hydrogen acceptor functionality on oxide surfaces can improve the catalytic performance for OER beyond the limitations originating from the scaling relations. We use this concept to search for promising combinations of binding sites and hydrogen donor/acceptor sites available in transition metal doped graphene, which can act as a catalyst for ORR and OER. We find that MnN4-site embedded in graphene by itself or combined with a COOH is a promising combination for a great combined ORR/OER catalyst.

1. Introduction

Energy conversion between free energy in the form of electricity and free energy bound in chemical fuels is a central part of any future renewable energy scenario. The so-called hydrogen economy combining the energy storage in energetically useable hydrogen, generated via water electrolysis with energy release in hydrogen fuel cells represents the most compelling of these scenarios. In practical terms the hydrogen economy scenario combines two technological devices – water electrolyzer and fuel cell.

Water electrolyzers consist of a cathode where protons are reduced to hydrogen gas and an anode where water is oxidized to oxygen [1], which is an unavoidable byproduct. Electrolyzers typically employ rare metal such as Pt or Pt alloys as cathode catalyst [1–3] and oxide based anode. The most common anodes are based on oxides of Ru, Ir and Ti and are usually described as Dimensionally Stable Anodes (DSAs) [4]. The performance of the state-of-the-art electrolyzers is controlled by the anodic oxygen production, since in contrast to the cathode reaction – (production of hydrogen) there are no catalysts that can oxidize water without requiring a substantial driving force. Therefore, the Oxygen Evolution Reaction (OER) is the main contributor to the electrolyzers' overpotential. Furthermore, the conditions for OER are rather harsh and so far known active catalysts for OER are fundamentally unstable in acid. Development of an active, efficient and stable catalyst for OER, represents, therefore, one of the major challenges in electrocatalysis [5,6].

The reverse of water electrolysis is electrochemical power generation in a hydrogen fuel cell. The fuel is oxidized at the anode while oxygen is reduced to water at the cathode. The cathode materials of choice are typically Pt [7,8] or Pt alloys with transition metals (such as Pt3Ni) or rare earth metals [9,10]. Similarly to the

* Corresponding author.
E-mail address: jan.rossmeisl@chem.ku.dk (J. Rossmeisl).

http://dx.doi.org/10.1016/j.nanoen.2016.04.011
2211-2855/

water electrolyzers the oxygen reduction reaction (ORR) is the main source of the power loss in a fuel cell [11]. The dream catalyst would be able to catalyze both OER and ORR close to the equilibrium potential. This would in principle alloy for efficient OER and ORR catalysis in the same devise, so called regenerative fuel cells working as both fuel cell and electrolyzers.

It has been previously established that the overpotentials are related to OER and ORR being 4-electrons reactions involving at least three intermediates along the reaction pathway [7,12]. All the intermediates have to bind with exactly the right strength to the surface to get the ideal catalysis of OER and ORR. It is evident, that to optimize simultaneously the binding of all the involved intermediates on a single catalyst surface may be an impossible task. It turns out that by controlling only the surface reactivity it is impossible to optimize the binding of one of the intermediates without compromising the binding of the others [29]. This is also discussed in paper by Herranz et al. and Zeng and Greeley in this Electrocatalysis Special Issue [34,35].

To increase the performance of existing catalyst materials or to find alternatives both reactions are subjects of intense research. Based on experimental and computational work several alternative water oxidation catalysts using abundant cobalt or manganese oxides [13–16] has been proposed. Improvements beyond the activity of the pure oxides has been obtained by mixing with other transition metals [17–19]. Similarly the presence of small amounts of Au mixed cobalt or manganese oxides was shown to result in significant improvements of the activity [20–22].

For the ORR transition metal and nitrogen doped graphenes (Me-N-C) [23–29] are studied extensively, also in this Special Issue [30–33], as potential non-precious oxygen reduction catalysts. In the latter case it has been suggested that contamination by traces of metals is the reason for their activity towards ORR [36]. So far, only in a few cases a catalytic activity for the OER has been discussed for these Me-N-C catalysts [37,38].

In the present study we have developed a combined model for both the OER and ORR based on recent mechanistic insights. Firstly, we assume that the binding of all intermediates can be controlled independently. Then we explore the limitations imposed by general linear scaling relationships, which are known to exist between the reactions' intermediates [39]. We find that control over at least two independent parameters is needed to optimize the catalysis. We then suggest a model system which provides these two independent, tunable parameters. We perform a computational screening applying Density Functional Theory (DFT) calculations for Mn, Fe and Co and nitrogen (Me-N4) embedded in graphene, combined with different hydrogen transfer moieties (NH_2, OH, graphene-H and COOH). We suggest promising combinations as potential ORR/OER catalysts. We only focus on the catalytic activity and the influence of the hydrogen transfer moeity and neglect the systems' stability.

2. Results and discussions

OER and ORR can be viewed as two reversed sequences of the same four coupled proton and electron charge transfer processes listed below as reactions (1)–(4). All the included elementary reactions are written in the oxidation direction. The mononuclear ORR and OER mechanisms proceeds via *–OH,*=O and *–OOH intermediates.

$$^{*}+H_2O \rightleftharpoons {}^{*}\text{–}OH+H^{+}+e^{-} \quad (1)$$

$$^{*}\text{–}OH \rightleftharpoons {}^{*}=O+H^{+}+e^{-} \quad (2)$$

$$^{*}=O+H_2O \rightleftharpoons {}^{*}\text{–}OOH+H^{+}+e^{-} \quad (3)$$

$$^{*}\text{–}OOH \rightleftharpoons {}^{*}+H^{+}+e^{-}+O_2 \quad (4)$$

From these reactions the individual reaction energies are given by:

$$\Delta G_1 = G_{OH} \quad (5)$$

$$\Delta G_2 = G_O - G_{OH} \quad (6)$$

$$\Delta G_3 = G_{OOH} - G_O \quad (7)$$

$$\Delta G_4 = G_{O2} - G_{OOH} \quad (8)$$

To ensure that each of the individual steps proceed spontaneously additional driving force needs to be provided. This additional driving force can be viewed as a potential, which needs to be applied to enable a given reaction step and will here be addressed as the potential. This is the computational hydrogen electrode model and in this framework there is no barrier for the proton transfer [7]. In the case of reaction sequence(s) (1)–(4) we can assume that the potential of the individual steps results from the differences in binding energy of the different intermediates before and after a charge is transferred. The entire ORR and OER are controlled by the reaction step requiring the highest driving force. This means that the potential limiting step for the OER is the maximum of reaction energies, ΔG_{1-4}, while in the case of the ORR it represents the minimum of the reaction energies, ΔG_{1-4}. The ideal electrocatalyst needs no driving force to catalyze the reactions, this means that all reaction energies are exactly equal to 1.23 eV, which is the equilibrium potential for OER/ORR.

Unifying the theoretical approach for OER and ORR we assume that all the reaction energies, ΔG_{1-4}, can be tuned independently with the only constraint that the binding of *–OH is equal to half the binding of *=O. This means that Eq. (9) is valid for 33 out of 52 of the oxides considered [39], 46 out of 60 metals and alloys considered [40] and for 14 out of 18 possible Me-N4 sites considered in this study within a ± 0.2 eV margin. It is therefore not impossible for a single site to be the perfect catalyst for both reactions (1) and (2). This can be written as:

$$\Delta G_1 = \Delta G_2 \quad (9)$$

$$\Delta G_1 + \Delta G_1 + \Delta G_3 + \Delta G_4 = 4.92 \text{ eV} \quad (10)$$

$$\Delta G_4 = 4.92 \text{ eV} - \Delta G_3 - 2\Delta G_1 \quad (11)$$

We can write the potentials for ORR and OER as:

$$U^{ORR} = \text{Min}\left[\Delta G_1, \Delta G_2, \Delta G_3, \Delta G_4\right]/e \quad (12)$$

$$U^{OER} = \text{Max}\left[\Delta G_1, \Delta G_2, \Delta G_3, \Delta G_4\right]/e. \quad (13)$$

With the relations (9)–(11), U^{ORR}, (12) and U^{OER}, (13), become functions of two independent parameters e.g. ΔG_1 and ΔG_3. We note that (Eqs. (12) and 13) are independent on the reaction path the only statement is that the reactions consist of four steps each related with a proton and electron transfer. The reaction (1)–(4) is a good choice of intermediates that have shown to described the potential limitations for both reactive and more noble catalysts. The energy landscapes for the ORR (blue pyramid) and OER (green pyramid) based on these simplifications are shown in Fig. 1. This three dimensional plot (Fig. 1(a)) shows that the perfect catalyst is represented by the common vertices of both pyramids. However, this also means that both ΔG_1 and ΔG_3 has to have exactly the right value.

The major obstacle in the catalysts optimization is the interdependence of the binding of the intermediate of the first and the

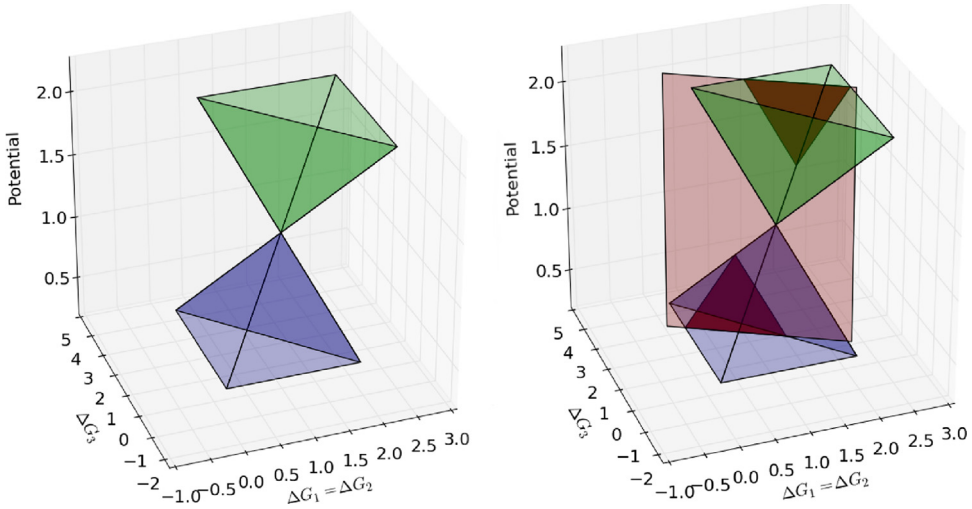

Fig. 1. Two pyramids which depict the best achievable potential for the ORR (blue) and the potential of the potential determining step for the OER (green) as a function of the first and the third reaction free energies. The constraint set by the constant offset of 3.2 eV between *–OH and *–OOH is represented by the red plane. The red plane that cuts the two pyramids creating two separate volcanoes for OER and ORR which are darkened. (For interpretation of the references to color in this figure legend, the reader is referred to the web version of this article.)

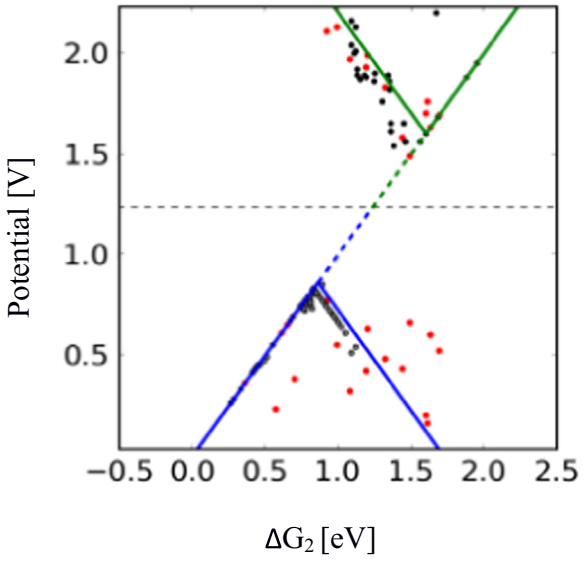

Fig. 2. 2D cross section represented by the red plane in Fig. 1 with the ORR (blue) and OER (green) volcano. The black dotted line visualizes the optimal potential of 1.23 eV for both ORR and OER. The ORR data for metals and alloys in gray are obtained from the literature [40] considered for the oxygen reduction reaction, OER data for oxides in black obtained from [39] and Me-N-C catalyst in red considered for both the ORR and OER which are listed in SI. (For interpretation of the references to color in this figure legend, the reader is referred to the web version of this article.)

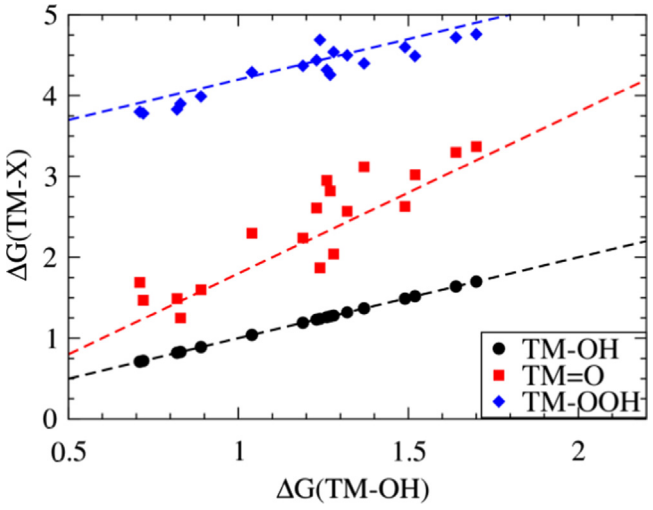

Fig. 4. A comparison between predictions from linear scaling relations for *–OH. *=O and *–OOH intermediates and the results obtained for different TM-N-C sites. TM is either Co, Fe or Mn.

third electron/proton transfer step, i.e. of *–OH and *–OOH. To tune ΔG_1 and ΔG_3 the binding of *–OH and *–OOH has to be tuned independently. This is impossible as the difference in energy of these intermediates is constant on simple surfaces and equal to ca. 3.2 eV [12,39]. Keeping in mind that the entire electrode process has an energy change of 4.92 eV (i.e. 1.23 eV for each electron/

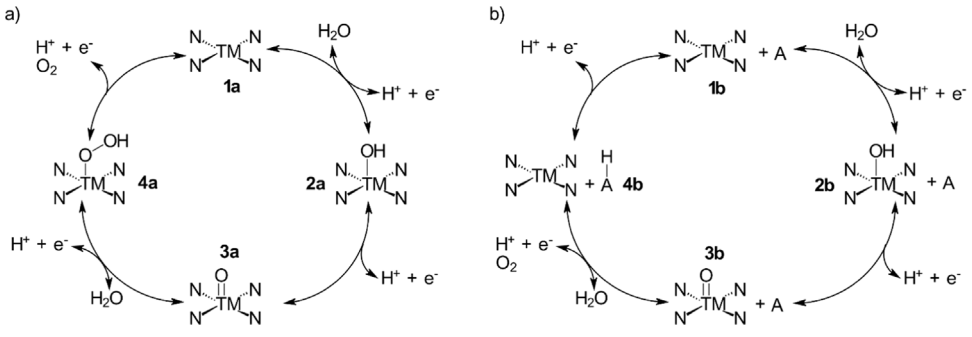

Fig. 3. (a) The catalytic cycle for OER clock wise and ORR anti clock wise at a single site TM and (b) the catalytic cycle including a hydrogen acceptor/donor site A nearby the TM site.

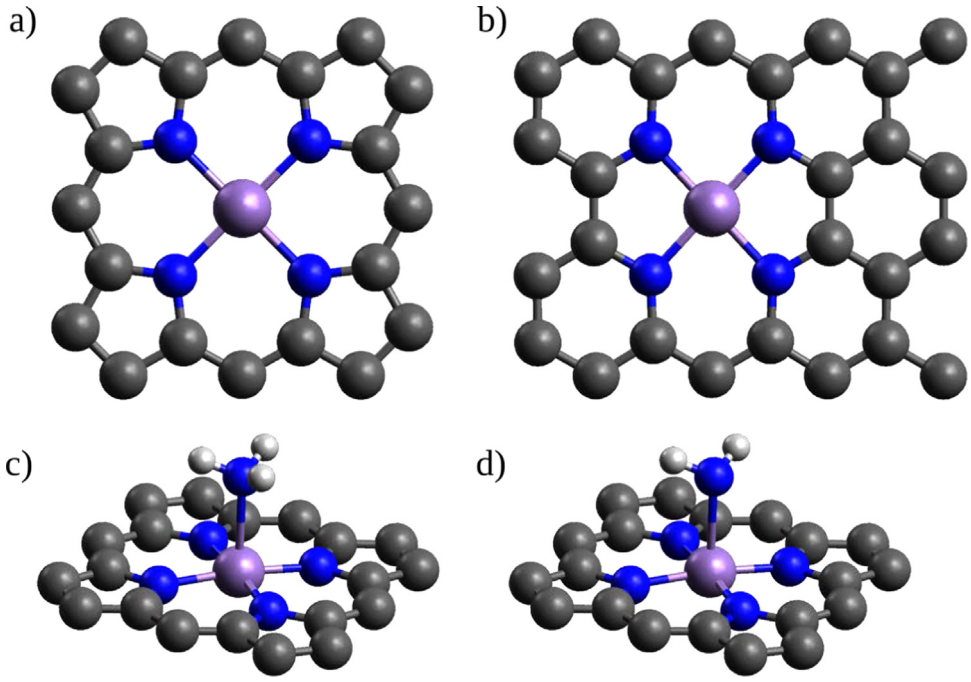

Fig. 5. The different types of Me-N-C sites used in this study with either pyrrolic coordination (a) or pyridnic coordination (b). The influence of a trans standing amino (c) and amido (NH_2) (d) ligand is also modelled here visualized in a pyrrolic embedding.

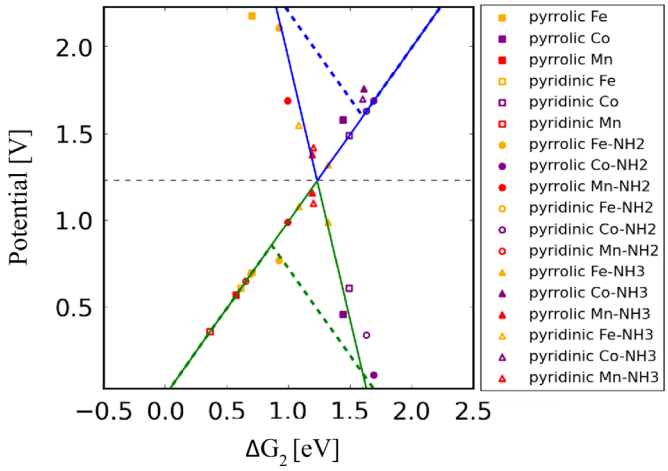

Fig. 6. ORR (green) and OER (blue) volcanoes using a secondary active site as a proton donor (ORR) or acceptor (OER) group. Within these approximations the thermodynamic limit of 1.23 V is theoretically achievable and some catalysts approach this limit. The volcanos based on the scaling between *–OH and *–OOH is shown for comparison in dashed lines. (For interpretation of the references to color in this figure legend, the reader is referred to the web version of this article.)

proton transfer step) the interdependence of the first and third intermediate imposes a severe restriction on the catalyst optimization. It means that the minimum average energy for reaction (2) and (3) is at least 1.6 eV (3.2 eV/2). As the energy difference between each of the four intermediate ideally should be 1.23 eV a minimum overpotential of at least ~0.4 V is obtained for both OER and ORR. Therefore, scaling relations between *–OH and *–OOH prevent any compound with a single site mechanism to be a perfect catalyst for either the OER or the ORR.

The linear scaling relations between *–OH and *–OOH dictate that catalysts surfaces can exist only in a subspace of the energy landscape represented by the two pyramids in Fig. 1. This subspace is illustrated in Fig. 1 as the plane intersects both pyramids based on the premise that $\Delta G_1 + 3.2\ eV = \Delta G_3 + 2\Delta G_1$. The boundaries of this cross section form the volcano curves for OER and ORR. This graphical representation clearly outlines two facts:

1) The apexes of the OER and ORR volcanos deviate from the position of the apex of the pyramids suggesting that a large driving force is needed even on the best catalysts (fulfilling the scaling relation) for each of the considered processes.
2) The apexes of the ORR and OER volcanos appear at different values for ΔG_1 and ΔG_3, which means that a good catalyst on the top of volcano for e.g. ORR is not a good catalyst for OER.

These two features are direct consequences of the scaling relations. This means that there is a forbidden region between the two volcanos and the perfect reversible ORR and OER catalyst (the apex of the two pyramids in Fig. 1) is in this forbidden region.

The consequences for eletrolyzers and fuels cells are that a high overpotential is needed to obtain a high current density. It also means that for catalysts limited by the scaling relation is it impossible to find a material that can work as both electrolyzer anode and fuel cell cathode without compromising the efficiency compared to electrolyzers and fuel cells separately.

Two volcanos are shown in Fig. 2 with data obtained from literature for the OER (green) [39] and the ORR (blue) [40] and the Me-N-C catalysts (red) considered in this study. The x-axis for the two volcanos is chosen to capture the potential limiting step which is in this case is ΔG_2. This is an unconventional descriptor for the ORR as ΔG_1 is usually the chosen descriptor. However, metal surfaces do not suffer from the same scatter in binding of *=O as oxides and Me-N-C catalysts do so chose of descriptor have little to no influence on the predicted overpotentials since as $\Delta G_1 = \Delta G_2$.

Most real catalysts are to be found on these two volcanos. For ORR a close comparison between the experimental and the theoretical volcano has been done on well-ordered single crystal faces of Pt, PtCu and Pt_3Ni alloys [41]. For OER experimental work in both the groups of Shao-Horn [17] and Jaramillo [42] have seen the same potential limits and the shape of the double volcano. Molecular analogs to the presented Me-N-C catalysts have also been

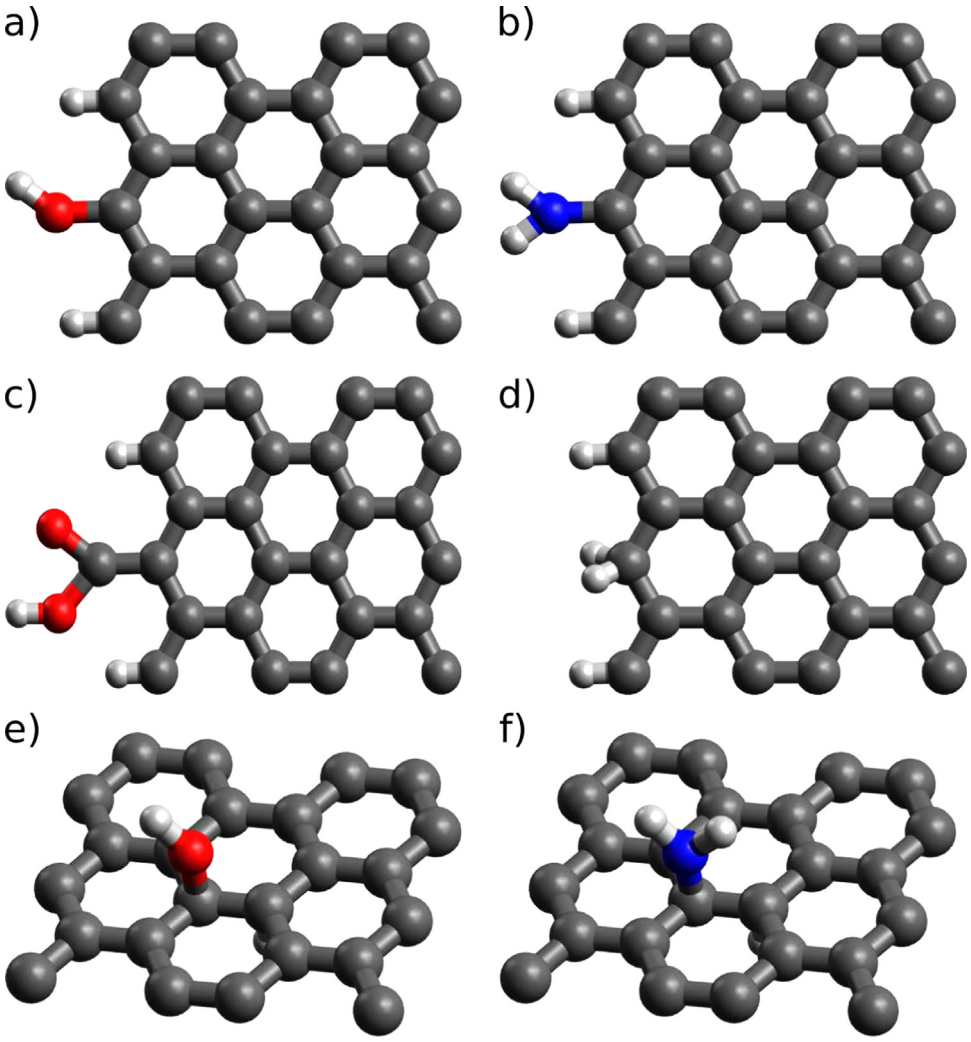

Fig. 7. Functionalised graphene sheet considered as hydrogen transfer moieties. (a) R-OH in plane (b) R-NH_2 in plane (c) R-COOH in plane (d) R-H2 on the edge (e) R-OH out of plane (f) R-NH_2 out of the plane. The R-H_2 is a special case as it is positioned at the edge, but the H is not in the plane of the graphene sheet.

analyzed using a double volcano analysis [43]. The interesting challenge that remains is to find a system capable of catalysis in the region between the ORR and OER volcanos, apparently forbidden by the scaling relations.

The restriction imposed from scaling relations may be bypassed introducing an alternative OER/ORR mechanism involving a combined catalytic site. For Fe-N-C catalysts it was reported that the catalytic activity for the ORR was significantly enhanced by providing protons during ORR from NH^+-sites in the vicinity of the FeN4-sites [44]. In addition to this, it has recently been demonstrated that Ni modified RuO_2 [45] and later for Au doped Mn and Co oxides [46] may bypass the scaling relations by avoiding the problematic *–OOH intermediate. DFT calculations identified Ru-O-Ni μ-oxo bridges or Au=O moieties acting as H acceptor units. The induced hydrogen acceptor functionality places the Ni and Co RuO_2 based catalysts as well Au doped MnO_2 catalysts into the region forbidden by the scaling relations in Fig. 2. Confined spaces where some intermediates can bind to multiple sites have in simulations shown the same functionality [47]. This, in principle, bypasses the major obstacle preventing reaching the ideal catalysts for both the ORR and OER as defined above.

Adopting the possible hydrogen transfer into the oxygen evolution mechanism requires the presence of a second surface site to complement the oxygen intermediates:

$$^*{=}O + A + H_2O \rightleftharpoons {}^* + A{-}H + O_2 + {}^* + H^+ + e^- \quad (14)$$

where A denotes a fully independent site that can accept the hydrogen and * denotes the oxygen binding site. The functionality of both sites is needed and they combine into an active site of the OER and ORR. This combined active site can reduce the overpotential for catalysts residing on the strong binding branch of the OER volcano (which are limited by formation of the *–OOH intermediate (ΔG_3)). This may push the overpotentials of the OER below the 0.4 eV limit. The catalytic cycles for the single site and combined sites are shown in Fig. 3a and b respectively.

The beneficial effect on the ORR and OER is illustrated in Fig. 3 (an example of energy diagrams is shown in Fig. 12). In case of water oxidation the first reaction steps resulting in the formation of *–OH and *=O are not influenced by the availability of a hydrogen acceptor unit. This is in contrast to *–OOH. In the presence of a suitable acceptor A the reaction may directly proceed from *=O to the formation of O_2 under reduction of A to A-H. The driving force for this reaction is the significantly higher stability of O_2+A-H compared to *–OOH. This alternative reaction path allows the reaction to proceed at a lower overpotential as it effectively avoids the potential determining formation of *–OOH. Similarly allow hydrogen donors for the direct breaking of the O-O bond during the first step of the ORR. This results in the formation of

Table 1
The redox potentials of the considered transition metal-free protonable functional groups are summarised. PyrroleH4 and PyridineH4 correspond to the fully reduced metall free Pyrrolic and Pyridinic sites while Pyrrole and Pyridine correspond to maximally oxidized Pyrrolic and Pyridinic sites. The structures of PyrroleHn and PyridineHn are shown in the SI.

Free pyridinic graphene		
System	Position	ΔG_{ox} (eV)
Pyridine-H_4 → PyridineH$_3$ + 0.5H_2		−0.40
Pyridine-H_3 → PyridineH$_2$ + 0.5H_2		−0.48
Pyridine-H_2 → PyridineH + 0.5H_2		1.91
Pyridine-H → PyridineH + 0.5H_2		2.16
Free pyrrolic graphene		
Pyrrole-H_4 → PyrroleH$_3$ + 0.5H_2		0.69
Pyrrole-H_3 → PyrroleH$_2$ + 0.5H_2		0.59
Pyrrole-H_2 → PyrroleH + 0.5H_2		1.97
Pyrrole-H → PyrroleH + 0.5H_2		2.59
Other organic hydrogen donors		
R-OH → R-O$^•$ + 0.5H_2	out of plane	1.65
	in plane	−0.60
R-NH_2 → R-NH$^•$ + 0.5H_2	Out of plane	2.52
	In plane	0.56
R-COOH → R-COO$^•$ + 0.5H_2	Out of plane	CO_2 desorbs
	In plane	1.05
R-H_2 → R-H + 0.5 h_2		1.14

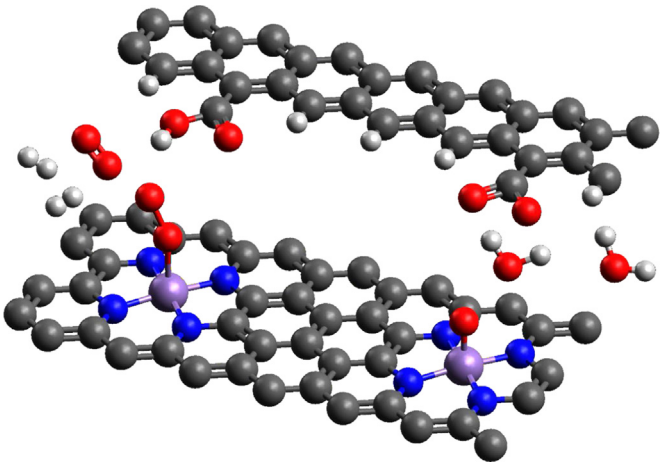

Fig. 8. Illustration of the concept of the specific region in which a MnN4-sites with pyridinic N-coordination adsorbing O containing species while an in-plane carboxylic acid in the vicinity is acting as a protonable group. This particular motif has a very promising activity as bifunctional catalyst for both OER and ORR.

*=O and an oxidized donor A. Accordingly the overpotential of the ORR may be decreased for catalysts at the weak binding side of the volcano as this alternative reaction route avoids the potential determining reduction of O_2 to *–OOH. Generally the H-acceptor/donor should be chosen such that its redox potential is close to the ideal 1.23 eV in order to avoid the recovery of the acceptor/donor unit to become potential determining.

The Me-N-C catalysts offer an ideal toolbox as they allow for relatively simple variation of binding sites (*) and independent hydrogen donor and acceptor sites (A). We use a test set comprising Me-N4 sites (Me=Fe, Co and Mn) with pyrrolic and pyridinic coordination, to vary the nature of the oxygen binding site *-sites, combined with a set of independent H acceptor/donor, A, sites.

The DFT calculations show that the behavior of the binding sites alone complies with the scaling relations restrictions

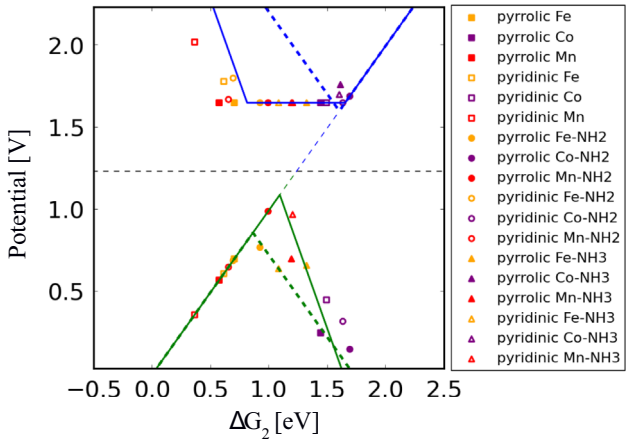

Fig. 9. The influence of introducing the out of plane facing R-OH hydrogen transfer moiety in the vicinity of a MeN4 sites embedded in graphene sheets and the resulting change of the volcanos for the OER (blue) and ORR (green). The volcanos based on the scaling between *–OH and *–OOH is shown for comparison in dashed lines. (For interpretation of the references to color in this figure legend, the reader is referred to the web version of this article.)

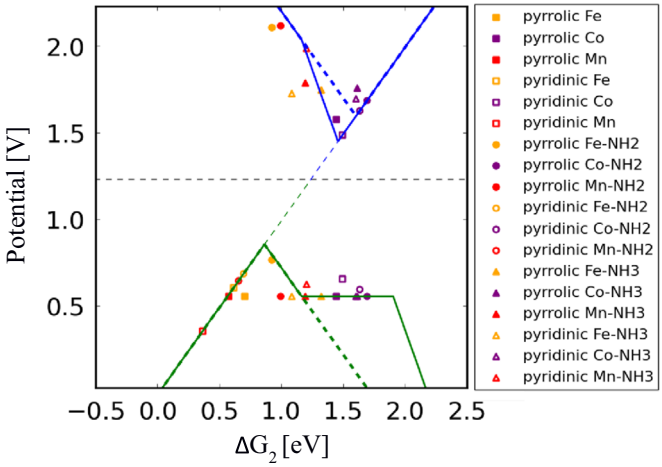

Fig. 10. The influence of introducing the in plane R-NH_2 hydrogen transfer moiety on a graphene sheet in the vicinity of a MeN4 sites and the resulting change of the volcanos for the OER (blue) and ORR (green). The volcanos based on the scaling between *–OH and *–OOH is shown for comparison in dashed lines. (For interpretation of the references to color in this figure legend, the reader is referred to the web version of this article.)

predicted for the binding of the *–OOH intermediate (see Fig. 4). The deviations from the scaling relation for *–OH and *–OOH is of the order of 0.1 eV. The calculated binding energies for *=O show some deviations from the scaling relations, which is well known for oxides [39] and for Me-N-C [27]. The binding sites * behave, therefore, in the conventional manner as other catalyst surfaces.

One possible scenario is that a that an additional protonable ligand binds to the Me-N-C site through a nitrogen atom close to the active site [49,50]. While such a ligand could certainly act as a hydrogen donor unit it might also be interpreted as a sixth ligand bound to the active site resulting in an octahedral coordination sphere. In the present study this additional ligand is modeled by a trans standing ammonia ligand as shown in Fig. 5. The potentials at which OER and ORR proceeds, an oxidation of ammonia to an amino group may be possible. This possibility was checked for all considered structures. Further oxidation of the *–NH_3 to *–NH_2 resulted in higher overpotentials required for OER and ORR in all cases.

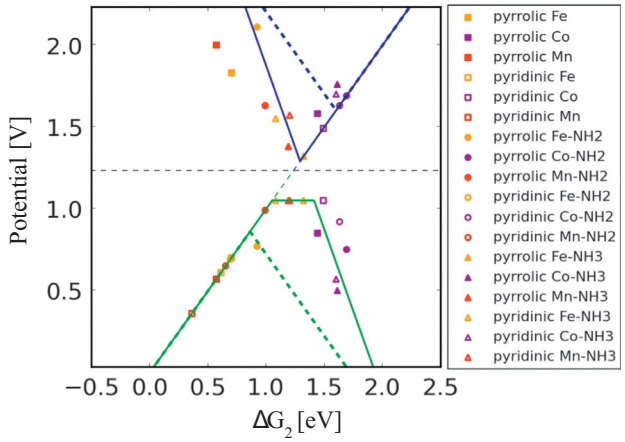

Fig. 11. The influence of introducing the in plane R-COOH hydrogen transfer moiety on a graphene sheet in the vicinity of a MeN4-sites embedded in graphene sheets and the resulting change of the volcanos for the OER (blue) and ORR (green). The volcanos based on the scaling between *–OH and *–OOH is shown for comparison in dashed lines. (For interpretation of the references to color in this figure legend, the reader is referred to the web version of this article.)

We now combine the functionalities of *-sites and A-sites. As a first example we use a second active site, HO–* and O=*, as hydrogen donor and acceptor respectively. This means that one should imagine two *-sites close to each other so that a hydrogen can be transferred. The resulting volcano is shown in Fig. 6 and is compared with the volcano based on scaling between *–OH and *–OOH with dashed lines. This binuclear mechanism has in principle no thermodynamic overpotential, but it requires that the two active sites are arranged in a very specific manner. Furthermore the secondary active site is potentially blocked for hydrogen transfer due to its own catalytic activity for the mononuclear mechanism [46]. Although the theoretical assessment of the catalytic activity of the Me-N-C sites may suggest a high activity, their application may be hindered by practical considerations (e.g. catalysts stability at the conditions of the OER) which are not involved in the analysis reflected in Fig. 6.

The active site described here closely resembles the Pacman molecules which have been investigated for ORR activity [51]. In Fig. 6 in is see that ORR volcano (limited by the scaling relation) is dominated by Fe containing sites, whereas the OER volcano top is dominated by Co. The best sites for the combine the functionality, however, is dominated by Mn. This supports the general finding that FeN4 site are good for ORR, and that Co based oxides are a fair OER catalyst. However, the findings here suggests that for the combined sites and thereby to go beyond the limitations put forward by the scaling relations, Mn is the best candidate.

However, due to the heterogeneous composition in the Me-N-C catalysts there are several possibilities for hydrogen transfers. Various functional groups can form during synthesis. Among others free pyrrolic and pyridinic sites as well as carboxy groups, hydroxy groups and amino groups may be formed (see Fig. 7). Additionally the conjugated π-system may be partially reduced. The redox properties of several likely donor sites are summarized in Table 1. Due to their unfavorable redox potentials neither free pyrrolic nor free pyridinic sites are expected to have a significant beneficial influence by acting as H acceptor or donor sites.

Organic functional groups either facing in-plane or out-of-plane on a nearby graphene sheet can serve as a protonable group which would allow for a breaking of the scaling between the *–OH and *–OOH. The calculated redox-potentials for the considered H donor/acceptor, A, sites is shown in Table 1. The in-plane facing R-COOH and partially hydrogenated C-C double bonds are found to show the most favorable redox potentials (i.e. potentials close to 1.23 eV) among all considered systems. An illustration of the model systems for the considered as likely protonable groups that can act as a protonable group which can influence the OER and/or ORR is shown in Fig. 7. These system have a molecular analog in the form of the hangman porphyrins which also been investigated for ORR activity [52]. Similarly also the trans standing Me-NH_2 /Me-NH_3 groups could act as H-donors or acceptors. Indeed favorable energetics are found for bare Pyrrolic and Pyridinic Fe-NH_3 /Fe-NH_2 as well as for bare and *–OH covered Pyrdinic Mn-NH_3 /Mn-NH_2. In reality however these sites may not be available as the transition metal itself acts as active site for OER and ORR (Fig. 8).

Common to all these protonable groups is that their redox potentials are independent of the metal ion in the Me-N-C site. The thermodynamic overpotential now depends on the binding of *=O to the Me-N-C site and the redox potential of the hydrogen donor group, A. The hydrogen transfer to an auxillary protonable group is also interesting as they in acidic electrolyte do not serve as a catalytic site for ORR and OER themselves and thereby don't reduce the number of active sites and are not blocked by the intermediates of the ORR and OER. The concept of the active site for either ORR or OER with MeN4 sites embedded in graphene adsorbing the O containing species and a nearby protonable group is illustrated in Fig. 9.

We plot the results for in-plane R-OH, R-NH_2 and R-COOH and the resulting change in the theoretical limits in Figs. 9, 10 and 11 respectively.

The in-plane R-OH functional group binds H too weakly to increase the activity of OER catalysts beyond the apex of the volcano which give a large flat region where the potential is limited by the

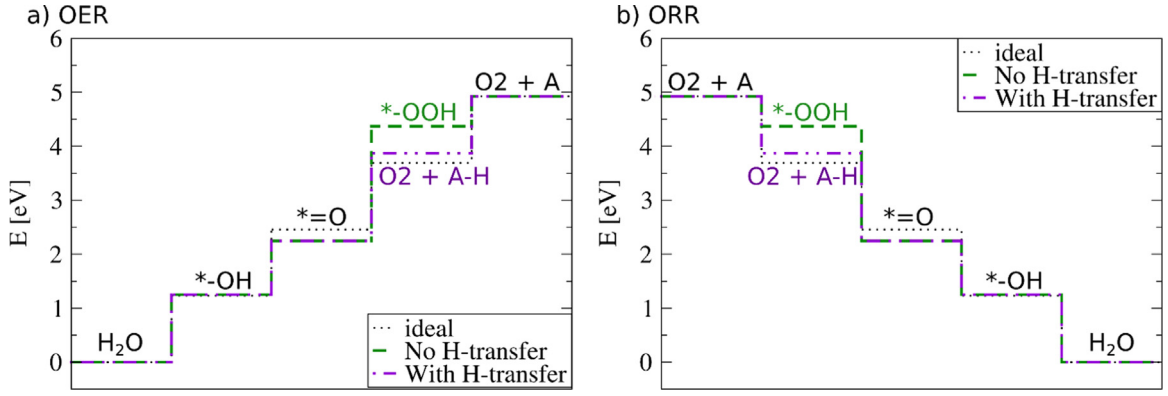

Fig. 12. Free energy diagrams for Pyrrolic Mn-NH_3 are depicted assuming a mechanism without H-transfer and H-transfer to/from a R-COOH group.

redox potential of the acceptor site of the protonable groups. ORR catalysts can benefit from protonable groups and achieve lower overpotentials than the 0.4 V limit predicted by a mononuclear OER/ORR reaction mechanism, see Fig. 9.

R-NH_2 in contrast binds H too strongly and therefore only OER catalysts can be improved beyond the 0.4 V limit. Still a sizable increase in activity can be achieved for otherwise poor catalysts, see Fig. 10.

A more suitable hydrogen transfer moiety is the in plane R-COOH which is significantly stabilized by the aromatic ring system compared to the out-of-plane equivalent. Fig. 11 show that both OER and ORR can obtain activities beyond the 0.4 V overpotential. OER catalysts benefit slightly more as the overpotential for the ORR catalyst ends up being limited by the slightly too low redox potential of the hydrogen transfer moeity.

In conclusion from this analysis it is evident that a protonable group in the vicinity of an active site for the OER or ORR could potentially lower the thermodynamic overpotential. In this case this is exemplified using MeN4-sites embedded in graphene sheets with various functional organic groups.

In Fig. 12 the energy diagrams for Pyrrolic Mn-NH3 with and without H-transfer to/from a R-COOH group is seen for both ORR and OER. It is seen that the energies are very close to the ideal reversible catalyst.

3. Computational details

To evaluate the activity of the different Pyrrolic and Pyridinic Me-N-C sites simplified model systems were constructed (see Fig. 4). Pyrrolic Me-N-c sites were modeled using a cubic unit cell with 8.335 Å × 8.335 Å and 20 Å in z direction. Pyridinic transition metal doped graphene was modeled using a 8.58 Å × 9.907 Å unit cell with 20 Å in z-direction. All DFT calculations were performed using the GPAW (version: 0.9.0.8965) [53,54] at the Generalized Gradient Approximation (GGA) level of theory using the RPBE functional [55]. The core electrons were modeled by Projector Augmented Wavefunctions (PAWs) [56] (build: 0.9.9672). A $2 \times 2 \times 1$ k-points set in combination with a 0.15 Å grid spacing was employed. Convergence tests were performed for pyrrolic Fe-N4-graphene. Increasing the accuracy to a $4 \times 4 \times 1$ k-point set or a 0.1 Å grid spacing resulted only in minor changes in the binding energies of the oxo and hydroxo intermediate. Spin was treated explicitly for all systems and allowed to relax during the convergence of the wave function. The geometries were optimized using the BFGS algorithm as implemented into ASE (version: 3.6.0) [57]. The intermediates' binding energies used in the present study were calculated following a procedure from literature including the zero-point energies and entropy contributions [58]. The binding free energies and the influence of protonable groups on the overpotential for OER and ORR are available in the SI.

4. Conclusion

We have unified oxygen reduction and the oxygen evolution reactions in a simple picture. It shows that we need control over two independent binding energies to obtain the perfect reversible ORR/OER catalyst. However, the linear scaling relations between binding of HO–* and HOO* impose limitations. This gives rise to a double volcano for ORR and OER. There is a region in between that is forbidden by the scaling relations. Due to the scaling relation there are no catalysts on which ORR and OER can proceed without an overpotential. Furthermore, a good catalyst on the top of the volcano for ORR is not on the top of the OER volcano. These consequences of the scaling relations are also observed experimentally for both ORR and OER.

The reversible perfect catalyst for both ORR and OER would fall into the “forbidden region”. Previously, we have found that a hydrogen acceptor functionality on oxide surfaces can improve the catalytic performance for OER beyond the limitations from the scaling relations. We use this concept to search for promising combinations of binding sites and hydrogen donor/acceptor sites.

The model system is the active site of Me-N-C catalysts (MeN4 embedded in graphene) for binding site for oxygen and different possible hydrogen containing groups as hydrogen donor and acceptor. We find that among others MnN4-sites embedded in graphene by itself or combined with a COOH group nearby is very promising for both the OER and ORR if the system is sufficiently stable.

Acknowledgments

The project was supported by the Carlsberg foundation grant CF15-0165. UIK acknowledges financial support by the DFG (GSC 1070).

Appendix A. Supporting information

Supplementary data associated with this article can be found in the online version at http://dx.doi.org/10.1016/j.nanoen.2016.04.011.

References

[1] M. Carmo, D.L. Fritz, J. Mergel, D. Stolten, A comprehensive review on PEM Water electrolysis, Int. J. Hydrog. Energy 38 (12) (2013) 4901–4934.
[2] S. Trasatti, Work function, electronegativity, and electrochemical behaviour of metals - III. Electrolytic hydrogen evolution in acid solutions, J. Electroanal. Chem. 39 (1) (1972) 163–184.
[3] J. Greeley, T.F. Jaramillo, J. Bonde, I.B. Chorkendorff, J.K. Nørskov, Computational high-throughput screening of electrocatalytic materials for hydrogen evolution, Nat. Mater. 5 (11) (2006) 909–913.
[4] S. Trasatti, Electrocatalysis: understanding the success of DSA®, Electrochim. Acta 45 (15–16) (2000) 2377–2385.
[5] I. Katsounaros, S. Cherevko, A.R. Zeradjanin, K.J.J. Mayrhofer, Oxygen electrochemistry as a cornerstone for sustainable energy conversion, Angew. Chem. Int. Ed. Engl. 53 (1) (2014) 102–121.
[6] N.S. Lewis, Toward cost-effective solar energy use, Science 315 (5813) (2007) 798–801.
[7] J.K. Nørskov, J. Rossmeisl, A. Logadottir, L. Lindqvist, J.R. Kitchin, T. Bligaard, H. Jónsson, Origin of the overpotential for oxygen reduction at a fuel-cell cathode, J. Phys. Chem. B 108 (46) (2004) 17886–17892.
[8] H.A. Gasteiger, S.S. Kocha, B. Sompalli, F.T. Wagner, Activity benchmarks and requirements for Pt, Pt-alloy, and non-Pt oxygen reduction catalysts for PEMFCs, Appl. Catal. B Environ. 56 (1–2) (2005) 9–35.
[9] V.R. Stamenkovic, B. Fowler, B.S. Mun, G. Wang, P.N. Ross, C.A. Lucas, N. M. Marković, Improved oxygen reduction activity on Pt3Ni(111) via increased surface site availability, Science 315 (5811) (2007) 493–497.
[10] M. Escudero-Escribano, A. Verdaguer-Casadevall, P. Malacrida, U. Grønbjerg, B. P. Knudsen, A.K. Jepsen, J. Rossmeisl, I.E.L. Stephens, I. Chorkendorff, Pt5Gd as a highly active and stable catalyst for oxygen electroreduction, J. Am. Chem. Soc. 134 (40) (2012) 16476–16479.
[11] N. Markovic, H. Gasteiger, P.N. Ross, Kinetics of oxygen reduction on Pt(*hkl*) electrodes: implications for the crystallite size effect with supported Pt electrocatalysts, J. Electrochem. Soc. 144 (5) (1997) 1591–1597.
[12] M.T.M. Koper, Thermodynamic theory of multi-electron transfer reactions: Implications for electrocatalysis, J. Electroanal. Chem. 660 (2) (2011) 254–260.
[13] A.M. Mohammad, M.I. Awad, M.S. El-Deab, T. Okajima, T. Ohsaka, Electrocatalysis by nanoparticles: optimization of the loading level and operating pH for the oxygen evolution at crystallographically oriented manganese oxide nanorods modified electrodes, Electrochim. Acta 53 (13) (2008) 4351–4358.
[14] K.A. Stoerzinger, M. Risch, J. Suntivich, W.M. Lü, J. Zhou, M.D. Biegalski, H. M. Christen, T. Venkatesan, Y. Shao-Horn, Oxygen electrocatalysis on (001)-oriented manganese perovskite films: Mn valency and charge transfer at the nanoscale, Energy Environ. Sci. 6 (5) (2013) 1582.
[15] M.M. Najafpour, T. Ehrenberg, M. Wiechen, P. Kurz, Calcium manganese(III) oxides (CaMn2O4.xH2O) as biomimetic oxygen-evolving catalysts, Angew. Chem. Int. Ed. Engl. 49 (12) (2010) 2233–2237.

[16] M. Busch, E. Ahlberg, I. Panas, Water oxidation on MnO_x and IrO_x : why similar performance? J. Phys. Chem. C 117 (1) (2013) 288–292.
[17] J. Suntivich, K.J. May, H.A. Gasteiger, J.B. Goodenough, Y. Shao-Horn, A perovskite oxide optimized for oxygen evolution catalysis from molecular orbital principles, Science 334 (6061) (2011) 1383–1385.
[18] M. Busch, E. Ahlberg, I. Panas, Hydroxide oxidation and peroxide formation at embedded binuclear transition metal sites; TM=Cr, Mn, Fe, Co", Phys. Chem. Chem. Phys. 13 (33) (2011) 15062–15068.
[19] F. Song, X. Hu, Exfoliation of layered double hydroxides for enhanced oxygen evolution catalysis, Nat. Commun. 5 (2014).
[20] Y. Gorlin, C.-J. Chung, J.D. Benck, D. Nordlund, L. Seitz, T.-C. Weng, D. Sokaras, B.M. Clemens, T.F. Jaramillo, Understanding interactions between manganese oxide and gold that lead to enhanced activity for electrocatalytic water oxidation, J. Am. Chem. Soc. 136 (13) (2014) 4920–4926.
[21] B.S. Yeo, A.T. Bell, Enhanced activity of gold-supported cobalt oxide for the electrochemical evolution of oxygen, J. Am. Chem. Soc. 133 (14) (2011) 5587–5593.
[22] Z. Zhuang, W. Sheng, Y. Yan, Synthesis of monodispere $Au@Co_3O_4$ core–shell nanocrystals and their enhanced catalytic activity for oxygen evolution reaction, Adv. Mater. 26 (23) (2014) 3950–3955.
[23] M. Ferrandon, A.J. Kropf, D.J. Myers, K. Artyushkova, U. Kramm, P. Bogdanoff, G. Wu, C.M. Johnston, P. Zelenay, Multitechnique characterization of a polyaniline–iron–carbon oxygen reduction catalyst, J. Phys. Chem. C. 116 (30) (2012) 16001–16013.
[24] U.I. Kramm, I. Abs-Wurmbach, S. Fiechter, I. Herrmann, J. Radnik, P. Bogdanoff, New insight into the nature of catalytic activity of pyrolysed iron porphyrin based electro-catalysts for the Oxygen Reduction Reaction (ORR) in acidic media, ECS Trans. 25 (1) (2009) 93–104.
[25] I. Herrmann, U.I. Kramm, S. Fiechter, P. Bogdanoff, Oxalate supported pyrolysis of CoTMPP as electrocatalysts for the oxygen reduction reaction, Electrochim. Acta 54 (18) (2009) 4275–4287.
[26] J. Tian, A. Morozan, M.T. Sougrati, M. Lefèvre, R. Chenitz, J.-P. Dodelet, D. Jones, F. Jaouen, Optimized synthesis of Fe/N/C cathode catalysts for PEM fuel cells: a matter of iron-ligand coordination strength, Angew. Chem. 125 (27) (2013) 7005–7008.
[27] F. Calle-Vallejo, J.I. Martínez, J. Rossmeisl, Density functional studies of functionalized graphitic materials with late transition metals for oxygen reduction reactions, Phys. Chem. Chem. Phys. 13 (34) (2011) 15639–15643.
[28] E.F. Holby, C.D. Taylor, Control of graphene nanoribbon vacancies by Fe and N dopants: implications for catalysis, Appl. Phys. Lett. 101 (6) (2012) 064102.
[29] E.F. Holby, G. Wu, P. Zelenay, C.D. Taylor, Structure of Fe–N x–C defects in oxygen reduction reaction catalysts from first-principles modeling, J. Phys. Chem. C 118 (26) (2014) 14388–14393.
[30] Edward F. Holby And Piotr Zelenay "Linking Structure to Function: The Search for Active Sites in Non-Platinum Group Metal Oxygen Reduction Reaction Catalysts" (Nano Energy) (same special issue).
[31] Gang Wu, Ana Santandreu, William Kellogg, Shiva Gupta, Ogechi Ogoke, Hanguang Zhang, a Hsing-Lin Wang and Liming Dai "Carbon Nanocomposite Catalysts for Oxygen Reduction and Evolution Reactions: from Nitrogen Doping to Transition-Metal Addition" Nano Energy, http://dx.doi.org/10.1016/j.nanoen.2015.12.032.
[32] Gaixia Zhang, Régis Chenitz, Michel Lefèvre, Shuhui Sun, Jean-Pol Dodelet "Is iron involved in the lack of stability of Fe/N/C electrocatalysts used toreduce oxygen at the cathode of PEM fuel cells? Nano Energy, http://dx.doi.org/10.1016/j.nanoen.2016.02.038.
[33] Qingying Jiaa, Nagappan Ramaswamya,b, Urszula Tylus ET Al., Spectroscopic Insights into the Nature of Active Sites in Iron–Nitrogen–Carbon Electrocatalysts for Oxygen Reduction in Acidand the Redox Mechanisms" (Nano Energy) (same soecial issue).
[34] Juan Herranz, Julien Durst, Emiliana Fabbri, Alexandra Patru, Xi Cheng, Anastasia A. Permyakova, Thomas J. Schmidt, Interfacial Effects on the Catalysis of the Hydrogen Evolution, Oxygen Evolution and CO_2-Reduction Reactions for (co-)Electrolyzer Development" Nano Energy, http://dx.doi.org/10.1016/j.nanoen.2016.01.027.
[35] Zhenhua Zeng and Jeffrey Greeley "Characterization of oxygenated species at water/Pt(111)) interfaces based on consistent DFT energetics and XPS simulations" Nano Energy,.
[36] L. Wang, A. Ambrosi, M. Pumera, 'Metal-Free' catalytic oxygen reduction reaction on heteroatom-doped graphene is caused by trace metal impurities, Angew. Chem. 125 (51) (2013) 14063–14066.
[37] N.R. Sahraie, J.P. Paraknowitsch, C. Go, A. Thomas, P. Strasser, Noble-metal-free electrocatalysts with enhanced ORR performance by task-specific functionalization of carbon using ionic liquid precursor systems, J. Am. Chem. Soc. 136 (41) (2014) 14486–14497.
[38] Y. Zhao, K. Kamiya, K. Hashimoto, S. Nakanishi, Efficient bifunctional Fe/C/N electrocatalysts for oxygen reduction and evolution reaction, J. Phys. Chem. C 119 (2015) 2583–2588.
[39] I.C. Man, H.-Y. Su, F. Calle-Vallejo, H.A. Hansen, J.I. Martínez, N.G. Inoglu, J. Kitchin, T.F. Jaramillo, J.K. Nørskov, J. Rossmeisl, Universality in oxygen evolution electrocatalysis on oxide surfaces, ChemCatChem 3 (7) (2011) 1159–1165.
[40] V. Viswanathan, H.A. Hansen, J. Rossmeisl, J.K. Nørskov, Universality in oxygen reduction electrocatalysis on metal surfaces, ACS Catal. 2 (8) (2012) 1654–1660.
[41] A.S. Bandarenka, H.A. Hansen, J. Rossmeisl, I.E.L. Stephens, Elucidating the activity of stepped Pt single crystals for oxygen reduction, Phys. Chem. Chem. Phys. 16 (27) (2014) 13625–13629.
[42] C.C.L. McCrory, S. Jung, J.C. Peters, T.F. Jaramillo, Benchmarking heterogeneous electrocatalysts for the oxygen evolution reaction, J. Am. Chem. Soc. 135 (45) (2013) 16977–16987.
[43] J.D. Baran, H. Grönbeck, A. Hellman, Analysis of porphyrines as catalysts for electrochemical reduction of O_2 and oxidation of H_2O, J. Am. Chem. Soc. 136 (2014) 1320–1326.
[44] A. Zitolo, V. Goellner, V. Armel, M.-T. Sougrati, T. Mineva, L. Stievano, E. Fonda, F. Jaouen, Identification of catalytic sites for oxygen reduction in iron- and nitrogen-doped graphene materials, Nat. Mater. 14 (9) (2015) 937–942.
[45] N.B. Halck, V. Petrykin, P. Krtil, J. Rossmeisl, Beyond the volcano limitations in electrocatalysis - oxygen evolution reaction, Phys. Chem. Chem. Phys. 16 (27) (2014) 13682–13688.
[46] R. Frydendal, M. Busch, N.B. Halck, E.A. Paoli, P. Krtil, I. Chorkendorff, J. Rossmeisl, Enhancing activity for the oxygen evolution reaction: the beneficial interaction of gold with manganese and cobalt oxides, ChemCatChem 7 (1) (2015) 149–154.
[47] A.D. Doyle, J.H. Montoya, A. Vojvodic, Improving oxygen electrochemistry through nanoscopic confinement, ChemCatChem 7 (5) (2015) 738–742.
[49] J. Herranz, F. Jaouen, M. Lefèvre, U.I. Kramm, E. Proietti, J.-P. Dodelet, P. Bogdanoff, S. Fiechter, I. Abs-Wurmbach, P. Bertrand, T.M. Arruda, S. Mukerjee, Unveiling N-protonation and anion-binding effects on Fe/N/C-catalysts for O_2 reduction in PEM Fuel Cells, J. Phys. Chem. C Nanomater. Interfaces 115 (32) (2011) 16087–16097.
[50] U.I. Kramm, J. Herranz, N. Larouche, T.M. Arruda, M. Lefèvre, F. Jaouen, P. Bogdanoff, S. Fiechter, I. Abs-Wurmbach, S. Mukerjee, J.-P. Dodelet, Structure of the catalytic sites in Fe/N/C-catalysts for O2-reduction in PEM fuel cells, Phys. Chem. Chem. Phys. 14 (33) (2012) 11673–11688.
[51] G. Givaja, M. Volpe, M.A. Edwards, A.J. Blake, C. Wilson, M. Schroder, J.B. Love, Dioxygen reduction at dicobalt complexes of a Schiff base calixpyrrole ligand, Angew. Chem. Int. Ed. 46 (2007) 584–586.
[52] R. McGuire Jr., D.K. Dogutan, T.S. Teets, J. Suntivich, Y. Shao-Horn, D.G. Nocera, Oxygen reduction reactivity of cobalt(ii) hangman porphyrins, Chem. Sci. 1 (3) (2010) 411.
[53] J.J. Mortensen, Real-space grid implementation of the projector augmented wave method, Phys. Rev. B (Condens. Matter Mater. Phys.) 71 (3) (2005).
[54] J. Enkovaara, C. Rostgaard, J.J. Mortensen, J. Chen, M. Dułak, L. Ferrighi, J. Gavnholt, C. Glinsvad, V. Haikola, H.A. Hansen, H.H. Kristoffersen, M. Kuisma, A.H. Larsen, L. Lehtovaara, M. Ljungberg, O. Lopez-Acevedo, P.G. Moses, J. Ojanen, T. Olsen, V. Petzold, N.A. Romero, J. Stausholm-Møller, M. Strange, G. A. Tritsaris, M. Vanin, M. Walter, B. Hammer, H. Häkkinen, G.K.H. Madsen, R. M. Nieminen, J.K. Nørskov, M. Puska, T.T. Rantala, J. Schiøtz, K.S. Thygesen, K. W. Jacobsen, Electronic structure calculations with GPAW: a real-space implementation of the projector augmented-wave method, J. Phys. Condens. Matter 22 (25) (2010) 253202.
[55] B. Hammer, L. Hansen, J. Nørskov, Improved adsorption energetics within density-functional theory using revised Perdew–Burke–Ernzerhof functionals, Phys. Rev. B 59 (11) (1999) 7413–7421.
[56] P.E. Blochl, Projector augmented wave-method, Phys. Rev. B 50 (24) (1994) 17953–17979.
[57] (Atomic Simulation) Environment. [Online]. (Available): ⟨https://wiki.fysik.dtu.dk/ase/⟩.
[58] J. Rossmeisl, Z.W. Qu, H. Zhu, G.J. Kroes, J.K. Nørskov, Electrolysis of water on oxide surfaces, J. Electroanal. Chem. 607 (2007) 83–89.

Michael Busch is currently Postdoc in the Laboratory for Computational Molecular Design at the École Polytechnique Fédérale de Lausanne. He obtained his diploma in chemistry from Ulm University in 2008 and moved to the University of Gothenburg to pursue his PhD studies. After graduation in 2012 he became Postdoc in the theoretical catalysis group at the Department of Physics at the Technical University of Denmark. He is interested in electrocatalysis, electrochemical water splitting, homogeneous catalysis and first-principles modeling of reactions at surfaces and molecular catalysts.

Niels Bendtsen Halck is a postdoc currently at DTU Energy at the Tehcnical University of Denmark. Niels obtained his master degree from DTU Chemistry in 2011 and a Ph.D. degree in physics from DTU Physics under the supervision of Professor Jan Rossmeisl in 2015. Niels uses his understanding of electrochemistry and atomic scale simulations to predict and understand reaction mechanisms and the working principles of electrocatalysts. His work has focused on oxygen evolution and oxygen reduction reaction and catalysts for these reactions.

Ulrike I. Kramm Since 03/2015 Ulrike Kramm holds a professorship on catalysts and electrocatalysts at TU Darmstadt. Before Ulrike worked at the BTU Cottbus-Senftenberg and had a guest professorship at the TU Berlin, Institute for Chemical Engineering. She conducted her PhD studies and part of her postdoc at the Helmholtz-Zentrum Berlin. During this time, she also started her still ongoing collaboration with Jean-Pol Dodelet from INRS-EMT where she did part of her postdoc. Ulrike is coauthor of more than 30 papers, 3 book chapters and one patent. Her research focusses on the development and fundamental understanding of new catalysts for energy relevant reactions.

Dr. Samira Siahrostami is a postdoctoral research fellow at the SUNCAT Center for Interface Science and Catalysis, Department of Chemical Engineering in Stanford University. She received her PhD in physical chemistry from the University of Shiraz in 2011. Before, she worked as a postdoc at the Center for Atomic-scale Material Design (CAMd) at the Technical University of Denmark. Her research interests include the use of DFT techniques to understand the kinetics and thermodynamics of reactions on the surface of heterogeneous catalysts and in electrochemical systems such as batteries and fuel cells. She is coauthor of more than twenty publications in peer reviewed journals and co-inventor of one patent.

Petr Krtil is a Senior Scientist at the J. Heyrovsky Institute of Physical Chemistry, Academy of Sciences of the Czech republic in Prague since 1993. He holds master's degree in chemical technology (1990) from the Prague Institute of Chemical Technology and Ph.D. degree (1993) in physical chemistry from the J. Heyrovsky Institute of Physical Chemistry in Prague. Petr has coauthored of more than 80 publications in peer reviewed journals, co-invented 3 patents. His research interests include physical electrochemistry, electrocatalysis, electrochemical energy storage and rational design of inorganic materials.

Jan Rossmeisl is Professor of theoretical chemistry at Department of Chemistry and the Nano-Science center at Copenhagen University. Before Jan was an Associate Professor and group leader for the theoretical catalysis group at Department of Physics at the Technical University of Denmark He holds master's (2000) and Ph.D. (2004) degrees in physics from the Technical University of Denmark. Jan is coauthor of more than 110 publications in peer reviewed journals, co-inventor of 4 patents and co-founder of two startup companies Research interests include electrocatalysis, energy conversion, atomic scale simulations, rational interface design for catalysis.